

RESEARCH ARTICLE

Motor control of an insect leg during level and incline walking

Chris J. Dallmann^{1,2,*,#}, Volker Dürr^{1,2} and Josef Schmitz^{1,2,#}

ABSTRACT

During walking, the leg motor system must continually adjust to changes in mechanical conditions, such as the inclination of the ground. To understand the underlying control, it is important to know how changes in leg muscle activity relate to leg kinematics (movements) and leg dynamics (forces, torques). Here, we studied these parameters in hindlegs of stick insects (*Carausius morosus*) during level and uphill/downhill (± 45 deg) walking, using a combination of electromyography, 3D motion capture and ground reaction force measurements. We find that some kinematic parameters including leg joint angles and body height vary across walking conditions. However, kinematics vary little compared with dynamics: horizontal leg forces and torques at the thorax–coxa joint (leg protraction/retraction) and femur–tibia joint (leg flexion/extension) tend to be stronger during uphill walking and are reversed in sign during downhill walking. At the thorax–coxa joint, the different mechanical demands are met by adjustments in the timing and magnitude of antagonistic muscle activity. Adjustments occur primarily in the first half of stance after the touch-down of the leg. When insects transition from level to incline walking, the characteristic adjustments in muscle activity occur with the first step of the leg on the incline, but not in anticipation. Together, these findings indicate that stick insects adjust leg muscle activity on a step-by-step basis so as to maintain a similar kinematic pattern under different mechanical demands. The underlying control might rely primarily on feedback from leg proprioceptors signaling leg position and movement.

KEY WORDS: Insect walking, Slope, Electromyography, Kinematics, Ground reaction force, Joint torque

INTRODUCTION

The ability to adjust leg muscle activity to changes in the mechanical demands acting on the body is critical for stable walking. During walking, the mechanical demands can vary considerably from one situation to the next. For example, while the gravitational force pulls the body toward the surface during level walking, it pulls the body backward during uphill walking and forward during downhill walking. How is leg muscle activity adjusted to adequately propel and stabilize (balance) the body in these situations?

From insects to mammals, leg muscle activity is thought to be controlled via neural circuits in the central nervous system that integrate descending inputs from the brain and afferent inputs from the leg (Hooper and Büschges, 2017; Orlovsky et al., 1999; Pearson, 1995; Prochazka, 1996). One possibility is that descending inputs mediate distinct motor programs for inclines, for example by modifying muscle synergies (Janshen et al., 2017; Smith et al., 1998). Another possibility is that afferent inputs from leg proprioceptors adjust leg muscle activity on a step-by-step basis. For example, if leg extensors are loaded more during uphill walking and less during downhill walking, load feedback could reflexively activate leg extensors more or less strongly and thereby automatically account for changes in the inclination of the ground (Donelan et al., 2009; Gregor et al., 2006).

To understand the potential contribution of descending and afferent inputs to control, it is important to determine leg muscle activity together with leg kinematics (movements) and leg dynamics (forces, torques) during level and incline walking. These parameters may indicate whether a distinct motor program is used on inclines (Lay et al., 2006, 2007), or to what extent movement- and load-related afferent inputs from the leg can account for adjustments in muscle activity (Donelan et al., 2009; Gregor et al., 2006). Here, we studied these parameters in a freely walking insect.


Because of their accessible nervous and musculoskeletal systems, insects have served as important model systems for studying leg motor control during walking (Ayali et al., 2015; Bidaye et al., 2018; Büschges and Gruhn, 2007; Tuthill and Wilson, 2016; Zill et al., 2004). Previous studies on insects have examined inclination-dependent changes in leg muscle activity (cockroach: Larsen et al., 1995; locust: Duch and Pflüger, 1995), leg kinematics (ant: Seidl and Wehner, 2008; cockroach: Spirito and Mushrush, 1979; fruit fly: Mendes et al., 2014) or leg forces (ant: Wöhrle et al., 2017; cockroach: Goldman et al., 2006; stick insect: Cruse, 1976b). However, no study has combined all measurements. As a consequence, changes in parameters such as joint torques, which are closely related to load feedback (Dallmann et al., 2017), remain unknown. In addition, the different species, walking speeds and inclinations investigated make it difficult to compare measurements and draw conclusions about control.

Here, we approached this issue by combining electromyography (EMG) with 3D motion capture and ground reaction force measurements in stick insects walking freely on level ground and up and down inclines (± 45 deg). The sensorimotor control of stick insect legs is comparatively well studied (Bässler, 1983; Büschges and Gruhn, 2007; Dürr et al., 2018; Graham, 1985). Importantly, the long and unspecialized legs of stick insects permit analysis of leg kinematics (Theunissen and Dürr, 2013), leg dynamics (Dallmann et al., 2016) and leg muscle activity (Dallmann et al., 2017) during unrestrained locomotion. In this study, we focused on hindlegs, which are critical to propel the body and stabilize it above ground during level walking (Dallmann et al., 2016). To better understand how the leg motor system copes with different mechanical demands, we asked (1) whether stick insects use distinct kinematic patterns on

¹Department of Biological Cybernetics, Bielefeld University, Universitätsstraße 25, 33615 Bielefeld, Germany. ²Cognitive Interaction Technology Center of Excellence, Bielefeld University, Inspiration 1, 33619 Bielefeld, Germany.

*Present address: Department of Physiology and Biophysics, University of Washington, 1705 NE Pacific Street, Seattle, WA 98195, USA.

#Authors for correspondence (cdallmann@uni-bielefeld.de; josef.schmitz@uni-bielefeld.de)

 C.J.D., 0000-0002-4944-920X; V.D., 0000-0001-9239-4964; J.S., 0000-0003-2054-9124

inclines, (2) how walking on inclines affects the forces and torques produced by the leg, and (3) how changes in kinematics and dynamics relate to changes in leg muscle activity. Our results suggest that stick insects do not use distinct, inclination-specific motor programs but instead adjust leg muscle activity on a step-by-step basis so as to minimize changes in kinematics under different mechanical demands.

MATERIALS AND METHODS

Animals and experiment

We tested eight adult, female stick insects (*Carausius morosus* Sinety 1901) reared in a laboratory colony (body mass: 0.9 ± 0.1 g, mean \pm s.d.; body length without antennae: ~ 75 mm). Animals walked freely along a walkway (40×500 mm) with five integrated force plates (Fig. 1A). The walkway was either horizontal or inclined at $+45$ deg (uphill) or -45 deg (downhill). Five animals were equipped with motion-capture markers and an EMG backpack for kinematic and electromyographic analyses (Figs 2, 4 and 5). To maintain the same EMG signal quality within animals, all trials of a given animal were recorded on a single day. To increase the number of force plate measurements, three additional animals without an EMG backpack were tested on multiple days. Because all force plate measurements showed the same characteristics for a given walking condition, data from all animals were used for dynamic analyses (Fig. 3).

Motion capture and force measurements

Leg movements and single leg ground reaction forces (GRFs) were measured and analyzed as described previously (Dallmann et al., 2016; Theunissen and Dürr, 2013). Although the present study focused on hindlegs, we recorded movements of all six legs by attaching 18 small, lightweight motion-capture markers to the body and leg segments (marker diameter: 1.5 mm; marker mass: 4 mg). Three markers were glued to the metathorax, one to the mesothorax, one to the prothorax, one to the head, and one to each of the femur and tibia (Fig. 1A). Markers were tracked in 3D with a sampling rate of 200 Hz using an eight-camera motion-capture system (Vicon MX10 with T10 cameras, controlled by Nexus 1.8.5 software; Vicon, Oxford, UK). Horizontal and vertical GRFs of the right hindleg were measured with strain gauge-based force plates with a sampling rate of 6 kHz (5×5 mm contact area; Fig. 1A; Dallmann et al., 2016). Kinematic and GRF data were low-pass filtered with a zero-lag, fourth-order Butterworth filter using cut-off frequencies of 20 and 10 Hz, respectively. Joint kinematics and joint torques were calculated in Matlab (The MathWorks, Natick, MA, USA) using a 3D rigid link model of the leg (Dallmann et al., 2016). The three main leg joints – the thorax–coxa (ThC) joint, the coxa–trochanter (CTr) joint and the femur–tibia (FTi) joint – were modeled as hinges with one degree of freedom each (Fig. 1B). Touch-down and lift-off events of the hindleg were determined manually based on a synchronized side view video of the walkway (Fig. 1A), which was recorded with an additional digital video camera with a sampling rate of 100 Hz (Basler A602fc, Ahrensburg, Germany).

Muscle recordings

We recorded EMGs from the protractor and retractor coxae muscles of the right hindlegs (Fig. 1C). EMGs of each muscle were recorded with a pair of steel wires (50 μ m diameter, insulated except for the tips). Wires were implanted through small holes in the metathorax and held in place with dental glue. Correct electrode placement was verified using standard criteria including resistance reflex responses to imposed forward–backward movements of the leg around the

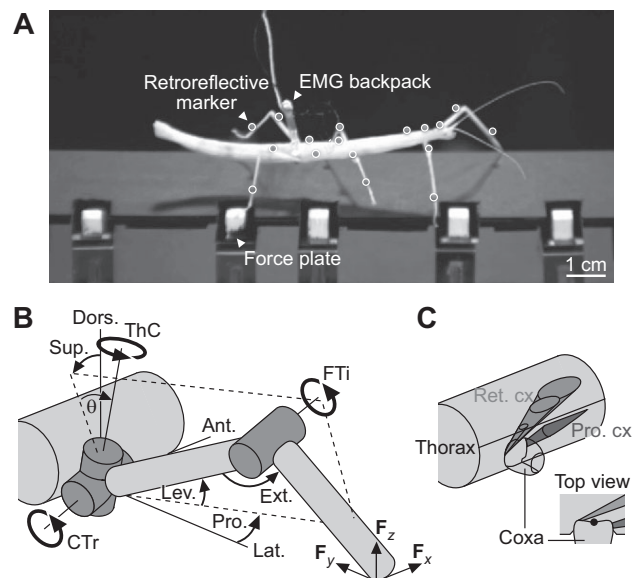


Fig. 1. Combining 3D motion capture, ground reaction force measurements and electromyography in freely walking stick insects.

(A) Side view of a stick insect carrying a lightweight EMG backpack and motion-capture markers (white circles) while stepping onto a force plate with its right hindleg. The walkway was either level (as shown here) or inclined at ± 45 deg. (B) Rigid link model of a right leg used for calculations of joint kinematics and torques (Dallmann et al., 2016). The thorax–coxa (ThC), coxa–trochanter (CTr) and femur–tibia (FTi) joints were modeled as hinges (dark gray). The ThC joint is slanted relative to the vertical body axis ($\theta = 30$ deg). The CTr joint is considered to be directly connected to the thorax. Leg segments indicate the tibia and an artificial segment comprising the coxa and the trochantero-femur (trochanter and femur are fused in stick insects). Positive torques about the ThC joint supinate (Sup.) and protract (Pro.) the leg. Positive torques about the CTr and FTi joint lift the coxa–trochantero-femur (Lev.) and extend the tibia (Ext.) within the leg plane (dashed lines), respectively. Leg forces (F) are shown in body-centered coordinates. Ant., anterior; Lat., lateral; Dors., dorsal. (C) EMGs were recorded from the protractor coxae (Pro. cx) and retractor coxae (Ret. cx) muscles of the hindleg in the metathorax. The protractor originates from the pleuron, inserts at the anterior rim of the coxa, and can move the leg forward; the retractor originates from the tergum, inserts at the posterior rim of the coxa, and can move the leg backward. Schematic diagram based on 2D drawings in Graham (1985).

ThC joint. Animals carried a lightweight EMG backpack (50 mg; Dallmann et al., 2017) to direct the EMG electrodes to the amplifiers without impairing leg movements. To affect overall body dynamics only minimally, the backpack was attached close to the body's center of mass (COM), which is located just behind the hindleg coxae (rear end of the fused metathoracic and first abdominal segment). Backpack attachment and electrode implantation had only small effects on joint kinematics (Fig. S1). Compared with control steps without an EMG backpack, average joint angles during swing and stance differed by less than 6 deg (Table S1). EMG signals were amplified and filtered with 50 Hz notch, 250 Hz high-pass, and 7.5 kHz low-pass filters using a custom-built amplifier (MA102, Electronics Workshop, Zoological Institute, Cologne, Germany). Filtered signals were A/D converted and recorded in parallel with Vicon Nexus and Spike2 (Cambridge Electronic Design, Cambridge, UK) with sampling rates of 6 kHz and 25 kHz, respectively. Vicon Nexus and Spike2 recordings were synchronized via a custom-built external trigger box.

The protractor and retractor EMGs were multiunit recordings (Fig. 4A). The protractor muscle is innervated by 6–9 excitatory motor neurons; the retractor muscles are innervated by up to 17

excitatory motor neurons (Goldammer et al., 2012). With the exception of large-amplitude protractor units (Fig. 4A,F), single units generally could not be discriminated. Therefore, we compared muscle activity across walking conditions based on rectified and low-pass filtered EMG signals. We used a first-order low-pass filter with a short time constant of 5 ms to accurately reflect the onset and offset of muscle activity. Rectified and smoothed EMG signals were divided into single step cycles (swing phase plus subsequent stance phase) based on the manually determined touch-down and lift-off events of the leg (see above). The minimum activity of each muscle per step cycle was set to zero. Typically, protractor activity was minimal during stance, whereas retractor activity was minimal during swing (Fig. 4A). To compare the time courses of muscle activity over the step cycle across walking conditions (Fig. 4B), swing and stance phases were time normalized to 1000 data points each and concatenated (see Fig. 2C for variability of stance and swing phase durations). To indicate changes relative to level walking, time courses from each animal were scaled to the mean magnitude of the animal's mean time course for level walking. To compare the magnitude of muscle activity across walking conditions (Fig. 4C,E), we took the integral of the EMG signal over each swing and stance phase. To indicate changes relative to level walking, the magnitude values from each animal were scaled to the animal's mean magnitude value for level walking. To better resolve the timing of muscle activity, we additionally thresholded the amplitude of the rectified and smoothed EMG signals for each step (Fig. 4A, dots above EMG traces). Pooled across trials, the times of muscle activity allowed us to calculate a likelihood of muscle activity relative to a given event, such as the touch-down of the leg (Fig. 4D). Careful inspection revealed that the retractor recording was occasionally contaminated by cross-talk from large-amplitude protractor potentials during swing. This cross-talk was edited out manually for likelihood calculations.

Statistical analysis

To test for the effect of inclination on kinematics and muscle activity while controlling for inter-animal differences, repeated measures and variations in walking speed, we used a linear mixed-effects model approach. The analysis was performed in R (<http://www.R-project.org/>) using the lme4 package (Bates et al., 2015). Kinematics and muscle activity were continuous response variables. We modeled each response variable as a function of the inclination of the walkway. The inclination was set as a categorical fixed effect with three levels (0, -45, +45 deg). We used dummy coding, with 0 deg as the baseline. Animals had random intercepts and random slopes for inclination and walking speed (mean speed of the COM over the step cycle). This way, the prediction of the response variable was allowed to differ for each animal, inclination and walking speed. Models were fitted with the restricted maximum likelihood method. Visual inspection of residual plots did not reveal any obvious deviations from normality or homoscedasticity (homogeneity of variance). To test for significance, we fitted each model to 1000 resampled datasets using parametric bootstrapping (bootMer function, lme4 package). This resulted in bootstrap distributions of the model coefficients for inclinations of -45 and +45 deg, for which we calculated the 95% confidence intervals (CI) (boot.ci function, percentile interval, boot package, <https://CRAN.R-project.org/package=boot>). If the CI of a model coefficient does not include zero, the corresponding inclination has a significant effect on the response variable at the 0.05 level. In Results, we report the model coefficients for inclinations of -45 and +45 deg (which indicate the difference from level walking), the corresponding

bootstrap CIs, and *P*-values obtained from the CIs as described by Altman and Bland (2011).

RESULTS

Kinematics are similar on inclines

To test whether stick insects use distinct kinematic patterns on inclines, we compared hindleg kinematics during level walking with those during uphill (+45 deg) and downhill (-45 deg) walking. Animals walked readily up and down the inclines. As in level walking, the hindleg closely followed the middle leg on the same side of the body, which in turn followed the front leg (Fig. 2B; see also Cruse, 1979; Dean and Wendler, 1983; Theunissen et al., 2014). Walking speeds ranged from 23 to 85 mm s⁻¹ (~0.3–1.1 body lengths s⁻¹; defined as the mean speed of the COM over the step cycle). In all walking conditions, stance duration of the hindleg decreased strongly with increasing walking speed, whereas swing duration varied little (Fig. 2C). The dependence of stance duration on walking speed was approximately hyperbolic as suggested previously for level walking insects (e.g. Larsen et al., 1995; Szczecinski et al., 2018; Wahl et al., 2015; Wendler, 1964). Stance duration tended to be longer on inclines (Fig. 2C, side boxplots). However, longer stance durations were correlated with slower walking speeds (Fig. 2C, top boxplots). After controlling for the effect of speed, inclination had no significant effect on stance or swing duration (swing duration: -45 deg, -0.003 s [-0.022, 0.018 s], coefficient [95% bootstrap CI], *P*=0.76; +45 deg, 0.002 s [-0.009, 0.013 s], *P*=0.78; stance duration: -45 deg, 0.013 s [-0.035, 0.056 s], *P*=0.58; +45 deg, 0.016 s [-0.024, 0.054 s], *P*=0.43). Accordingly, the hyperbolic fits of stance duration over walking speed were practically identical in all conditions (Fig. 2C, see legend for model fits).

Other kinematic parameters showed significant changes during incline walking, but most of them were comparatively small (Table 1). For example, the mean height of the COM tended to increase with increasing inclination, but only from 9.8 to 12.0 mm (Fig. 2D and Table 1; -45 deg, -1.6 mm [-3.0, -0.3 mm], *P*<0.05; +45 deg, 0.6 mm [-0.8, 1.9 mm], *P*=0.42). Similarly, the mean body pitch angle (angle between metathorax and walking surface) tended to decrease with increasing inclination, but only from 5.6 to 2.7 deg (Fig. 2E and Table 1; -45 deg, 0.7 deg [-0.5, 1.9 deg], *P*=0.25; +45 deg, -2.3 deg [-3.6, -1.3 deg], *P*<0.001). That is, the body was kept at a similar height and almost parallel to the walking surface in all conditions. Touch-down and lift-off positions of the hindleg were shifted anteriorly with increasing inclination (Fig. 2G, side boxplots; touch-down position: -45 deg, -1.1 mm [-1.7, -0.5 mm], *P*<0.001; +45 deg, 3.2 mm [1.9, 4.7 mm], *P*<0.001; lift-off position: -45 deg, -1.0 mm [-1.6, -0.5 mm], *P*<0.001; +45 deg, 0.7 mm [0.0, 1.5 mm], *P*=0.06). The change was largest for the touch-down position during uphill walking (3.4 mm or 16% step length on average, Table 1 and Fig. 2G, arrowhead). Accordingly, step length (distance between touch-down and lift-off position) was slightly increased for uphill walking (12% on average, Table 1 and Fig. 2F; -45 deg, -0.1 mm [-1.0, 0.8 mm], *P*=0.77; +45 deg, 2.6 mm [1.6, 3.5 mm], *P*<0.001).

Time courses of joint angles were similar across walking conditions (Fig. 2H). In all conditions, the leg protracted, supinated, levated and flexed during swing, and retracted, pronated, depressed and extended during stance. Compared with their range during level walking, average joint angles during swing and stance changed only a little on inclines (<17%; Table 1). With increasing inclination, the hindleg was more protracted at the end of swing (Fig. 2H, arrowhead; protraction at 100% swing: -45 deg,

–2.0 deg [–3.8, –0.3 deg], $P<0.05$; +45 deg, 10.1 deg [6.6, 13.8 deg], $P<0.001$). This was consistent with the shift in touch-down position. With increasing inclination, the hindleg tended to be less levated at the beginning of stance, and it was less extended at the end of stance (Fig. 2H, arrowheads; levation at 20% stance: –45 deg, 7.0 deg [4.4, 9.6 deg], $P<0.001$; +45 deg, –1.9 deg

[–4.0, 0.2 deg], $P=0.08$; extension at 80% stance: –45 deg, 18.2 deg [12.6, 24.1 deg], $P<0.001$; +45 deg, –11.6 deg [–16.5, –7.0 deg], $P<0.001$). The latter was consistent with the shift in lift-off position. These changes also affected the average joint angular velocity during swing and stance (Fig. 2I). For example, the velocity of the ThC joint during swing was increased for uphill

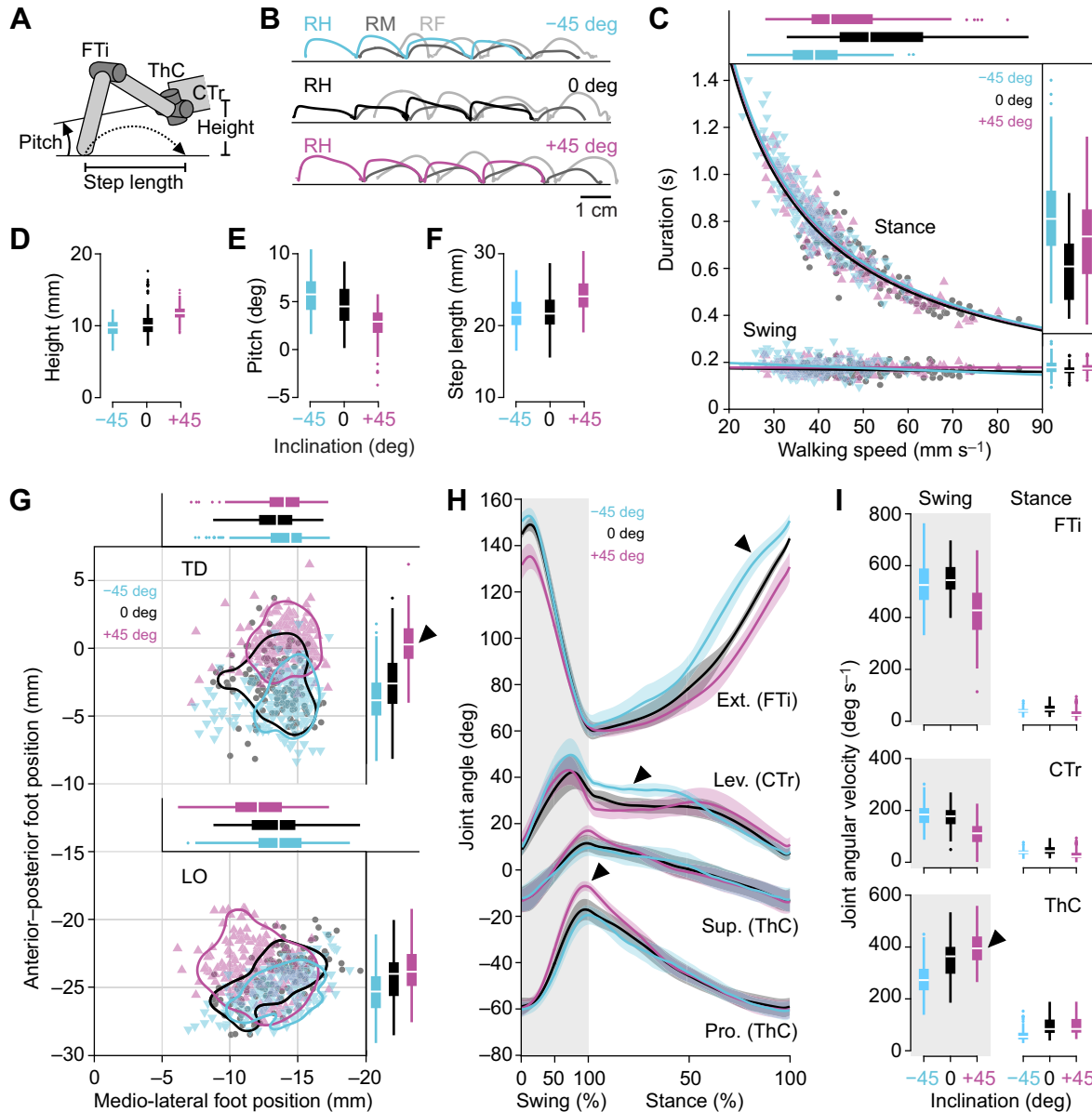


Fig. 2. Hindleg kinematics during level and incline walking. (A) Side-view schematic diagram of the rigid link model of the hindleg and metathorax. (B) Example side-view trajectories of the tibia–tarsus joint of a right hindleg (RH) during downhill walking (blue), level walking (black) and uphill walking (magenta). Dark gray and light gray lines show trajectories of the right middle leg (RM) and right front leg (RF), respectively. Walking direction is from left to right. (C) Stance and swing durations of the hindleg as a function of walking speed for downhill walking (blue), level walking (black) and uphill walking (magenta). Each data point corresponds to a swing or stance phase (–45 deg, 174 steps from 5 animals; 0 deg, 126 steps from 5 animals; +45 deg, 199 steps from 5 animals). Lines show hyperbolic fits of stance duration over speed (a/speed ; –45 deg, $a=31.32$, $R^2=0.83$; 0 deg, $a=30.27$, $R^2=0.78$; +45 deg, $a=31.02$, $R^2=0.89$) and linear fits of swing duration over speed ($a \times \text{speed} + b$; –45 deg, $a=-7 \times 10^{-4}$, $b=0.21$, $R^2=0.03$; 0 deg, $a=-2 \times 10^{-4}$, $b=0.18$, $R^2=0.01$; +45 deg, $a=7 \times 10^{-6}$, $b=0.18$, $R^2<0.01$). Boxplots show pooled data. (D–F) Body height, body pitch and step length as a function of inclination, pooled across the steps shown in C. (G) Touch-down (TD) and lift-off (LO) positions of the hindleg in body-centered coordinates. (0,0) marks the ThC joint. Contours indicate the 75th percentile ranges based on 2D kernel density estimates (Botev et al., 2010) of pooled steps. Boxplots also show pooled data. The arrowhead marks the maximal deviation in foot placement from level walking. Sample numbers as in C. (H) Joint angles of the hindleg normalized to swing and stance duration (see Fig. 1B for angle conventions). Lines and error bands show means and 95% confidence intervals of animal means (–45 deg, 5 animals, 19–45 steps per animal; 0 deg, 5 animals, 18–33 steps per animal; +45 deg, 5 animals, 19–55 steps per animal). Arrowheads mark the maximal angle deviations from level walking. (I) Angular velocities of the ThC, CTr and FTi joints during swing (left) and stance (right). Note that the ThC velocity is the first derivative of the angle describing the rotation of the leg plane around the slanted ThC joint axis (combined protraction and supination, see Fig. 1B). Sample numbers as in C.

Table 1. Kinematic parameters for level (0 deg) and incline (± 45 deg) walking

Kinematic parameter	-45 deg	0 deg	+45 deg
Body height (mm)	9.8 \pm 1.0 [-173]	11.1 \pm 2.6	12.0 \pm 1.0 [134]
Body pitch (deg)	5.6 \pm 1.6 [55]	4.8 \pm 1.6	2.7 \pm 1.2 [-142]
Step length (mm)	21.4 \pm 1.8 [-1]	21.6 \pm 2.4	24.2 \pm 1.5 [12]
TD anterior–posterior (mm)	-4.0 \pm 1.4 [-5]	-3.0 \pm 1.4	0.4 \pm 0.8 [16]
TD medial–lateral (mm)	-13.9 \pm 1.8 [-3]	-13.2 \pm 1.5	-13.6 \pm 1.4 [-2]
LO anterior–posterior (mm)	-25.3 \pm 1.3 [-4]	-24.3 \pm 1.4	-23.6 \pm 1.4 [4]
LO medial–lateral (mm)	-13.5 \pm 1.5 [-1]	-13.2 \pm 1.0	-11.9 \pm 1.7 [6]
Pro. swing (deg)	-41.7 \pm 3.8 [-7]	-38.6 \pm 2.8	-33.0 \pm 2.4 [13]
Pro. stance (deg)	-43.6 \pm 4.0 [-1]	-42.9 \pm 3.8	-41.4 \pm 3.2 [4]
Sup. swing (deg)	-0.9 \pm 5.0 [-3]	-0.2 \pm 5.1	1.6 \pm 4.1 [7]
Sup. stance (deg)	-0.2 \pm 5.2 [<1]	-0.1 \pm 4.6	0.0 \pm 4.1 [<1]
Lev. swing (deg)	36.6 \pm 6.0 [16]	30.9 \pm 6.5	32.9 \pm 5.9 [6]
Lev. stance (deg)	26.3 \pm 2.5 [8]	23.6 \pm 3.7	24.2 \pm 5.1 [2]
Ext. swing (deg)	111.4 \pm 4.8 [1]	110.2 \pm 5.5	102.3 \pm 2.0 [-9]
Ext. stance (deg)	96.7 \pm 5.2 [11]	86.8 \pm 3.5	80.9 \pm 3.3 [-7]
ThC velocity swing (deg s ⁻¹)	282.7 \pm 55.0 [-10]	346.7 \pm 61.2	387.4 \pm 36.6 [6]
ThC velocity stance (deg s ⁻¹)	61.1 \pm 19.4 [-5]	93.3 \pm 32.4	93.7 \pm 28.3 [<1]
CTr velocity swing (deg s ⁻¹)	183.7 \pm 24.1 [2]	173.4 \pm 13.8	105.6 \pm 26.0 [-12]
CTr velocity stance (deg s ⁻¹)	39.9 \pm 4.4 [-1]	46.7 \pm 10.6	27.3 \pm 12.5 [-3]
FTi velocity swing (deg s ⁻¹)	526.9 \pm 63.0 [-2]	548.7 \pm 17.5	423.2 \pm 50.6 [-10]
FTi velocity stance (deg s ⁻¹)	111.8 \pm 13.0 [-2]	143.0 \pm 24.3	102.4 \pm 28.8 [-3]

Values are means \pm s.d. of animal means (-45 deg, 5 animals, 19–45 steps per animal; 0 deg, 5 animals, 18–33 steps per animal; +45 deg, 5 animals, 19–55 steps per animal). Values in brackets indicate differences from level walking as a percentage of the range of the parameter (peak-to-peak amplitude of the parameter's mean time course) during the step cycle of level walking. In the case of step length and touch-down and lift-off positions, differences are expressed relative to the mean step length for level walking. Body height and body pitch are net values averaged over the step cycle. Angles and angular velocities of the thorax–coxa (ThC), coxa–trochanter (CTr) and femur–tibia (FTi) joints are net values averaged over each phase of the step cycle. TD, touch-down; LO, lift-off; Pro., protraction angle; Sup., supination angle; Lev., levation angle; Ext., extension angle. See Fig. 1B for angle conventions.

walking (Fig. 2I, arrowhead; -45 deg, -21.5 deg [-62.3, 20.8 deg], $P=0.32$; +45 deg, 46.9 deg [18.7, 75.3 deg], $P<0.01$), consistent with an increased protraction angle at the end of swing. Compared with its range during level walking, however, average joint angular velocity changed little on inclines (<13%; Table 1).

In summary, stick insects tended to walk slower on inclines with some changes in kinematics. Overall, however, the kinematic pattern was similar across walking conditions considering the range of kinematic parameters during the step cycle and the substantial changes in the inclination of the ground.

Leg forces and joint torques reveal substantial changes in mechanical demands on inclines

Because animals kept their body almost parallel to the walking surface, the orientation of the body with respect to gravity differed substantially across walking conditions. To study the consequent changes in the mechanical demand on the legs, we analyzed hindleg forces and joint torques during level and incline walking (Fig. 3 and Table 2). Forces and torques during level walking corresponded well with our previous measurements on level ground (Dallmann et al., 2016), but they differed substantially on inclines.

The hindleg pushed backward to accelerate the body during level and uphill walking, but it pushed forward to decelerate the body during downhill walking (Fig. 3B, F_x , arrowhead). The sign reversal during downhill walking was evident in all steps recorded. It was accompanied by a change in the medio-lateral direction, in which the hindleg reversed from pushing outward during uphill walking to pulling inward during downhill walking (Fig. 3B, F_y , arrowhead). Vertical forces were smaller during downhill walking (Fig. 3B, F_z), suggesting that the middle and front legs carried more body weight in this situation.

Changes in the anterior–posterior and medio-lateral force were primarily reflected in changes in torques at the ThC and FTi joints (Fig. 3C and Table 2). Torques at the ThC joint were directed toward

retraction during level and uphill walking but toward protraction during downhill walking (Fig. 3C, τ_{ThC} , arrowhead). Similarly, torques at the FTi joint were directed toward extension during uphill walking but toward flexion during downhill walking (Fig. 3C, τ_{FTi} , arrowhead). That is, torques at both joints were directed opposite to joint movement during downhill walking, which suggests a stabilizing function (Fig. 3D, gray shaded areas). Torques at the CTr joint differed less across conditions (Fig. 3C, τ_{CTr}). Torques at this joint generally reflected the vertical force of the leg and were directed toward joint movement (Fig. 3D, middle).

In summary, the changes in hindleg forces and joint torques reveal substantial changes in mechanical demands during incline walking, particularly at the ThC and FTi joints. The changes in dynamics are consistent with the animal's need to counteract the effects of gravity by accelerating the body more strongly during uphill walking and decelerating it during downhill walking.

Timing and magnitude of muscle activity are adjusted on inclines

The torques at the ThC and FTi joints indicated that muscle activity at these joints is adjusted in an inclination-dependent manner. However, as net torques represent the net magnitude and direction of all forces acting at the joint, it is not clear how a given net torque relates to the activity of any particular muscle. Therefore, we recorded EMGs of the protractor and retractor coxae muscles, which rotate the leg forward and backward around the ThC joint, respectively (Fig. 1C).

During swing, when the leg was mechanically uncoupled from the ground, the pattern of muscle activity was similar across walking conditions and reflected the forward movement of the leg. In all conditions, the protractor was active throughout swing, whereas the retractor was silent (Fig. 4A,B). Persisting protractor activity throughout swing is to be expected even during downhill walking, because the strong passive forces associated with the small mass of insect legs prevents leg inertia from completing swing movements

(Hooper et al., 2009). While the timing of protractor activity did not change across conditions, the magnitude of protractor activity tended to increase with increasing inclination (Fig. 4B,C, top; -45 deg, -0.07 [$-0.29, 0.17$], $P=0.58$; $+45$ deg, 0.58 [$0.25, 0.93$], $P<0.001$). The magnitude of muscle activity was only weakly correlated with the velocity of the ThC joint in individual steps (Fig. 4E, left, see legend for model fits). But faster joint velocities were correlated with an increased likelihood of occurrence of large-amplitude (putative fast) protractor units (Fig. 4F).

During stance, when the leg was mechanically coupled to the ground, the pattern of muscle activity was strongly dependent on the inclination of the walkway and did not directly reflect the backward movement of the leg. The protractor was strongly active during downhill walking, less active during level walking and essentially silent during uphill walking (Fig. 4A,B, arrowheads top). The magnitude of protractor activity tended to decrease with increasing inclination (Fig. 4B,C, top; -45 deg, 0.28 [$-0.08, 0.65$], $P=0.13$; $+45$ deg, -0.68 [$-0.82, -0.54$], $P<0.001$). Inclination-dependent changes of protractor activity occurred primarily in the first 50% of

stance (Fig. 4B, top). Close inspection revealed that this activity was not a continuation of the burst during swing, but a separate burst starting with touch-down of the leg (Fig. 4A,D, top). Conversely to protractor activity, retractor activity during stance generally increased with increasing inclination (Fig. 4A,B, arrowheads bottom, and Fig. 4C, bottom; -45 deg, -0.28 [$-0.37, -0.19$], $P<0.001$; $+45$ deg, 0.27 [$0.12, 0.41$], $P<0.001$). The muscle was strongly active during level and uphill walking, starting with touch-down of the leg. During downhill walking, the retractor was sometimes also briefly active with touch-down of the leg, but its main activity was reduced and delayed in all steps (~ 200 ms; Fig. 4B,D, bottom). Similar to protractor activity, inclination-dependent changes in retractor activity occurred primarily in the first 50% of stance (Fig. 4B, bottom).

The changes in protractor and retractor activity during stance generally reflected the changes in net torque at the ThC joint. That is, the net protraction torque during downhill walking corresponded to strong protractor and weak retractor activity, and the increasing net retraction torque from level to uphill walking corresponded to

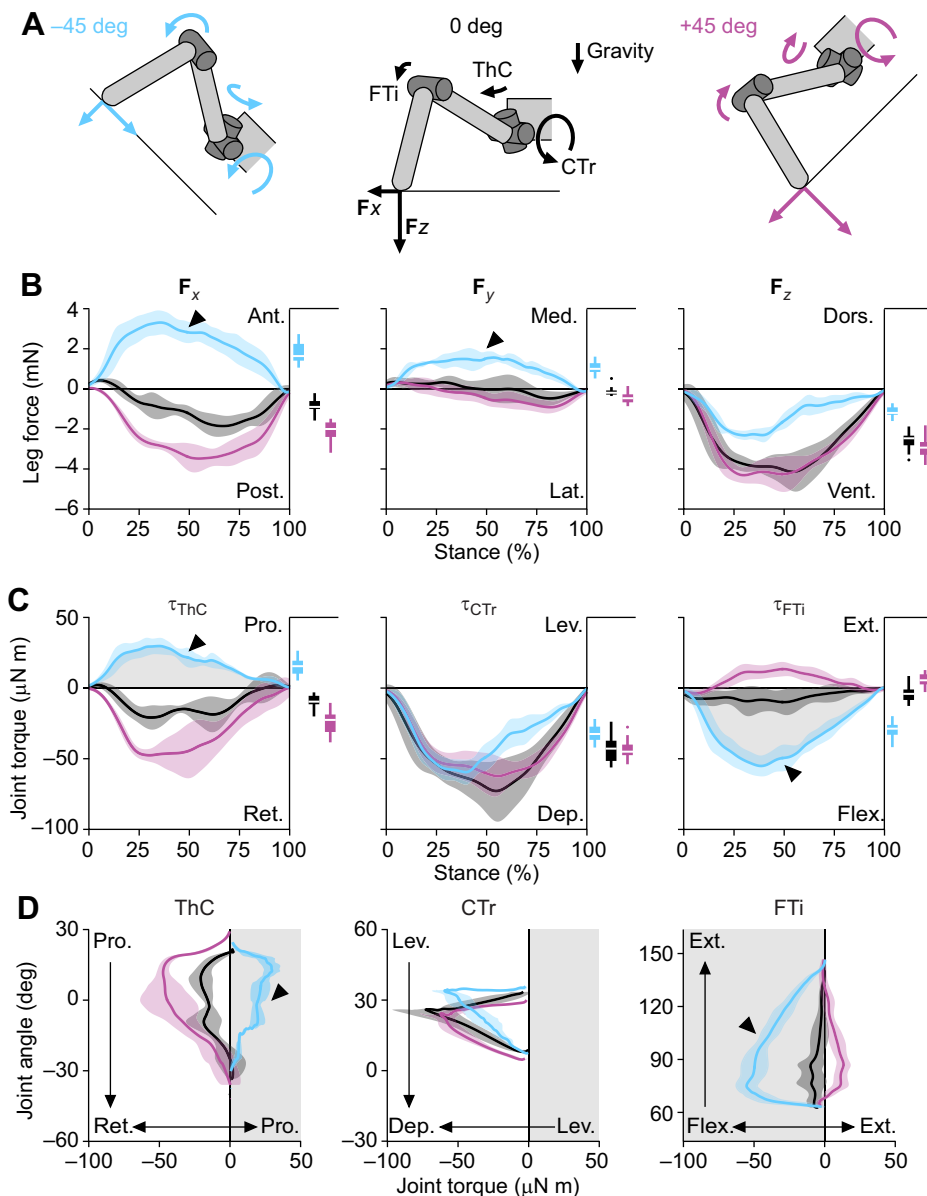


Fig. 3. Hindleg forces and joint torques during level and incline walking. (A) Side-view schematic diagrams of the rigid link model of the hindleg and metathorax, illustrating the average posture, forces and torques of the leg at 50% stance during downhill walking (blue), level walking (black) and uphill walking (magenta). Walking direction is from left to right. The center of mass (COM) of the body is located just behind the ThC joint. Note that the direction of forces and torques indicates the action of the leg, which is opposite to the direction of the ground reaction force (GRF). (B,C) Hindleg forces (B) and joint torques (C) normalized to the stance phase of downhill walking (blue), level walking (black) and uphill walking (magenta). Lines and error bands show means and 95% confidence intervals of animal means (-45 deg, 4 animals, 2–11 steps per animal; 0 deg, 4 animals, 1–8 steps per animal; $+45$ deg, 5 animals, 1–11 steps per animal). Boxplots show net forces and torques averaged over each stance phase, pooled across animals (-45 deg, 20 steps from 4 animals; 0 deg, 15 steps from 4 animals; $+45$ deg, 21 steps from 5 animals). Gray areas in C highlight stabilizing phases (see D). Arrowheads mark sign reversals for downhill walking. Note that there is no one-to-one correspondence between a given torque and any one force component. (D) Joint angles as a function of joint torques. Arrows indicate movement or torque directions during stance. Gray areas highlight stabilizing phases, in which the net joint torque is directed opposite to the movement of the joint. Arrowheads mark the stabilizing torques during downhill walking. Note that the ThC angle is the angle describing the rotation of the leg plane around the slanted ThC joint axis (combined protraction and supination, see Fig. 1B). Sample numbers as in B and C.

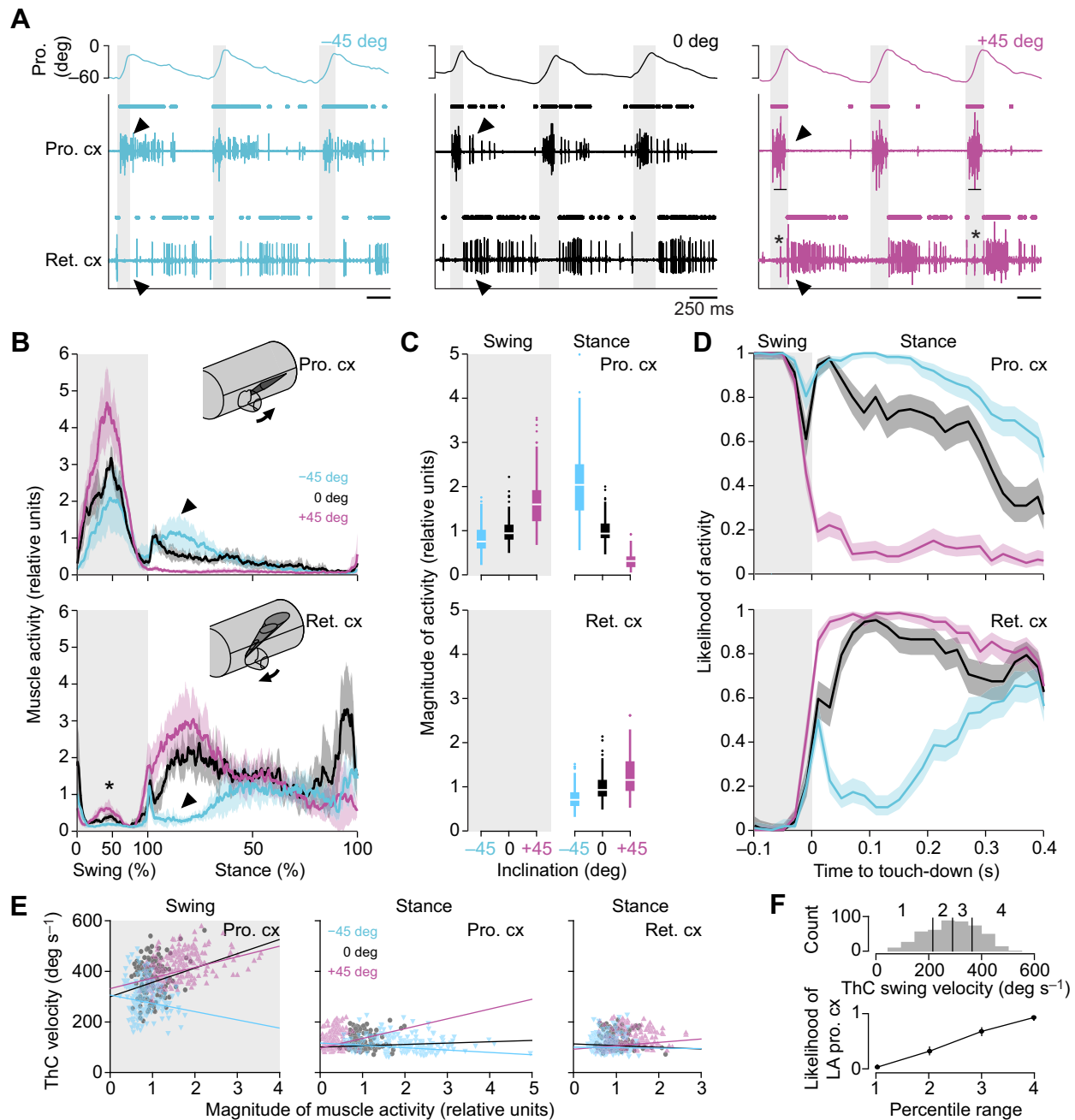


Fig. 4. Muscle activity at the ThC joint during level and incline walking. (A) Example EMG traces for the hindleg protractor coxae (Pro. cx) and retractor coxae (Ret. cx) muscles during downhill walking (blue), level walking (black) and uphill walking (magenta). Dots above EMG traces mark muscle potentials detected based on amplitude. Traces on top show the protraction angle of the leg around the ThC joint. Light gray rectangles mark swing phases. Arrowheads mark inclination-dependent changes in muscle activity at the beginning of stance. Asterisks in the retractor trace mark cross-talk from large-amplitude protractor potentials (right, truncated in protractor trace). (B) Average rectified and smoothed EMG traces of the protractor and retractor muscles normalized to the swing and stance phase of downhill walking (blue), level walking (black) and uphill walking (magenta). The magnitude of muscle activity is scaled to the mean magnitude for level walking (see Materials and Methods). Lines and error bands show means and 95% confidence intervals of animal means (−45 deg, 5 animals, 19–45 steps per animal; 0 deg, 5 animals, 18–33 steps per animal; +45 deg, 5 animals, 19–55 steps per animal). Arrowheads mark inclination-dependent changes in muscle activity at the beginning of stance. The asterisk marks protractor cross-talk during swing. (C) Magnitude of muscle activity during swing (left) and stance (right) scaled to the mean magnitude of the respective phase for level walking. Boxplots show pooled data (−45 deg, 174 steps from 5 animals; 0 deg, 126 steps from 5 animals; +45 deg, 199 steps from 5 animals). Note that the retractor was silent during swing. (D) Likelihood of muscle activity relative to leg touch-down. Lines and error bands show means and binomial 95% confidence intervals (Wilson score intervals) of pooled steps. Sample numbers as in C. Protractor cross-talk during swing was edited out manually. (E) ThC velocity as a function of the magnitude of muscle activity. Each data point corresponds to a swing or stance phase. Lines show linear fits of ThC velocity over protractor magnitude during swing (left; $a \times \text{magnitude} + b$; −45 deg, $a = -33$, $b = 307$, $R^2 = 0.02$; 0 deg, $a = 58$, $b = 298$, $R^2 = 0.05$; +45 deg, $a = 42$, $b = 333$, $R^2 = 0.15$), protractor magnitude during stance (middle; −45 deg, $a = -9$, $b = 118$, $R^2 = 0.05$; 0 deg, $a = 6$, $b = 100$, $R^2 < 0.01$; +45 deg, $a = 39$, $b = 97$, $R^2 = 0.04$) and retractor magnitude during stance (right; −45 deg, $a = -2$, $b = 100$, $R^2 < 0.01$; 0 deg, $a = -7$, $b = 113$, $R^2 < 0.01$; +45 deg, $a = 13$, $b = 94$, $R^2 = 0.02$). Sample numbers as in C. (F) Histogram of the velocity of the ThC joint during swing pooled across all steps (top) and likelihood of occurrence of large-amplitude (LA) protractor coxae muscle potentials as a function of the percentile range (bottom). Error bars show Wilson score intervals. Sample numbers as in C.

Table 2. Dynamic parameters for level (0 deg) and incline (± 45 deg) walking

Dynamic parameter	-45 deg	0 deg	+45 deg
F_x (mN)	2.1 \pm 0.5 [129]	-0.9 \pm 0.1	-2.3 \pm 0.3 [-61]
F_y (mN)	1.0 \pm 0.1 [123]	0.0 \pm 0.3	-0.3 \pm 0.2 [-39]
F_z (mN)	-1.2 \pm 0.1 [38]	-2.7 \pm 0.4	-2.9 \pm 0.4 [-5]
τ_{ThC} (μ N m)	16.5 \pm 2.7 [115]	-9.9 \pm 2.3	-26.8 \pm 6.5 [-74]
τ_{CTr} (μ N m)	-33.6 \pm 2.7 [18]	-46.4 \pm 10.3	-43.3 \pm 7.1 [4]
τ_{FTi} (μ N m)	-32.2 \pm 4.5 [-262]	-5.9 \pm 5.0	5.6 \pm 2.8 [115]

Values are means \pm s.d. of animal means (-45 deg, 4 animals, 2–11 steps per animal; 0 deg, 4 animals, 1–8 steps per animal; +45 deg, 5 animals, 1–11 steps per animal). Values in brackets indicate differences from level walking as a percentage of the average range of the parameter (peak-to-peak amplitude of the parameter's mean time course) during the stance phase of level walking. Forces (F) and torques (τ) are net values averaged over the stance phase. See Fig. 1B for force and torque conventions.

decreasing protractor and increasing retractor activity (see boxplots in Figs 3C and 4C). In contrast, the changes in protractor and retractor activity during stance did not directly reflect joint kinematics; the magnitude of muscle activity was only weakly correlated with the velocity of the ThC joint (Fig. 4E, middle and right, see legend for model fits).

In summary, both the timing and magnitude of antagonistic muscle activity at the ThC joint were adjusted to altered mechanical demands during incline walking. The changes in muscle activity during stance reflect changes in joint torques but not joint kinematics.

Muscle activity changes with the first step of the leg on the incline

Because the characteristic adjustments in muscle activity occurred primarily in the first half of stance immediately after touch-down of the leg, we wondered whether they are a reflexive response to altered

mechanical demands or whether they occur in anticipation of the incline, as reported for mammals (Gottschall and Nichols, 2011). To investigate this question, we recorded protractor and retractor activity in a stick insect transitioning from level to either downhill or uphill walking (Fig. 5). Fig. 5B shows that the characteristic adjustments in muscle activity observed during steady-state incline walking occurred as soon as the hindleg stepped on the incline. That is, with the first step of the hindleg on the -45 deg incline, protractor activity increased during early stance, whereas retractor activity was delayed (Fig. 5B, arrowheads left). Conversely, with the first step of the hindleg on the +45 deg incline, protractor activity decreased during early stance, whereas retractor activity increased (Fig. 5B, arrowheads right). These adjustments were not present in the steps preceding the transition (Fig. 5B, black traces). First adjustments occurred during the transition steps (Fig. 5B, gray traces). In these steps, the body pitch angle (and with that, the mechanical demand on the hindleg) was altered as the front and middle legs encountered the incline. Together, these data suggest that muscle activity was adjusted to the current mechanical demand on a step-by-step basis rather than in anticipation of the incline.

DISCUSSION

To better understand how leg motor systems cope with different mechanical demands during walking, we measured muscle activity, kinematics and GRFs in stick insect hindlegs during level and incline walking. Some kinematic parameters varied across walking conditions (Fig. 2 and Table 1). However, kinematics changed much less than leg forces and joint torques, which revealed substantial changes in mechanical demands (Fig. 3 and Table 2). At the ThC joint, the altered mechanical demands were met by characteristic adjustments in the timing and magnitude of antagonistic muscle activity, which occurred primarily in the first half of stance (Fig. 4) and with the first step of the leg on the incline (Fig. 5).

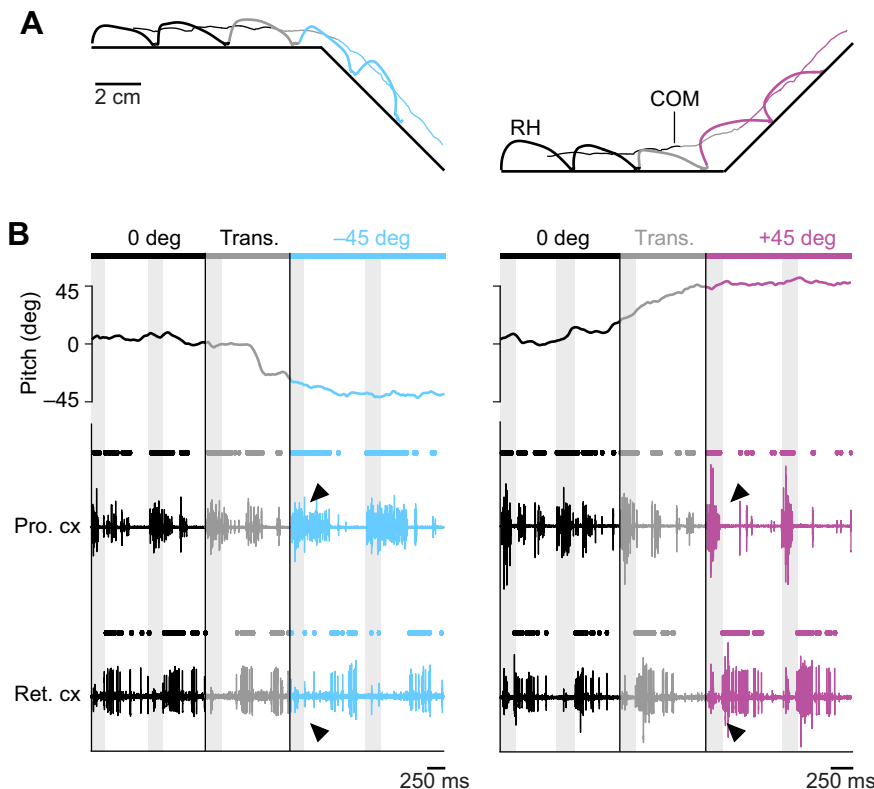


Fig. 5. Muscle activity at the transition from level to incline walking. (A,B) Example transitions from level to downhill walking (left) and level to uphill walking (right). Lines in A show side-view trajectories of the COM and the tibia-tarsus joint of the right hindleg (RH). EMG traces in B show activity of the hindleg protractor coxae and retractor coxae muscles. Dots above EMG traces mark muscle potentials detected based on amplitude. Protractor cross-talk during swing was edited out manually. Light gray rectangles mark swing phases. Transition (Trans.) steps, in which the body pitch angle is adjusted as front and middle legs encounter the incline, are dark gray. Steps before the transition are black, steps after the transition are blue (downhill) or magenta (uphill). Arrowheads mark characteristic, inclination-dependent changes in muscle activity at the beginning of stance.

Inclination-dependent changes in kinematics, dynamics and muscle activity

Stick insects tended to walk slower on the ± 45 deg inclines with some changes in kinematics (Fig. 2). Overall, however, kinematic parameters were similar across walking conditions considering their range during the step cycle (Table 1) and the substantial changes in the inclination of the ground. This is generally consistent with previous observations in insects (Mendes et al., 2014; Seidl and Wehner, 2008; Weihmann and Blickhan, 2009). For example, ants walking on ± 60 deg inclines do not adjust the touch-down and lift-off positions of their legs (Seidl and Wehner, 2008). Similarly, fruit flies walking vertically or upside-down show only minor adjustments in leg placement (Mendes et al., 2014). The situation is quite different in larger vertebrates. For example, cats and humans require consistent and strong kinematic adjustments for stable walking on inclines, including changes in body tilt, foot placement and inter-joint coordination (Carlson-Kuhta et al., 1998; Gregor et al., 2006; Lay et al., 2006; Leroux et al., 2002; Smith et al., 1998).

In contrast to kinematics, hindleg forces and joint torques varied substantially across walking conditions (Fig. 3). The largest changes concerned the anterior–posterior and medio-lateral directions, in which the hindleg reversed from pushing backward and outward during level and uphill walking to pushing forward and pulling inward during downhill walking. This sign reversal is consistent with the animal's need to control the descent of the body during downhill walking and was also described in ants (Wöhrle et al., 2017) and larger vertebrates (Gregor et al., 2006; Lay et al., 2006). In stick insects, the sign reversal was primarily reflected in changes in torques at the ThC and FTi joints. At these joints, torques were directed toward retraction and extension during uphill walking, but toward protraction and flexion during downhill walking. This result was not predicted from kinematics, because the leg was retracted and extended similarly in all conditions. This indicates that the ThC and FTi joints stabilized the leg during downhill walking, supporting our previous hypothesis that these two leg joints may serve a stabilizing function (Dallmann et al., 2016).

The inclination-dependent changes in antagonistic muscle activity at the ThC joint corroborate this hypothesis (Fig. 4). Strictly reciprocal activity of the protractor and retractor muscles reflecting the swing and stance phases of the leg was only present during uphill walking. In contrast, during level and downhill walking, the protractor muscle was active during the first half of stance. This resulted in periods of co-activation and probably considerable co-contraction with the retractor muscle given the long activation and deactivation time constants of insect muscle (Guschlbauer et al., 2007; Hooper et al., 2007; Zakotnik et al., 2006). The co-activation of antagonistic muscles indicates that the ThC joint was actively stiffened to stabilize the leg depending on the current mechanical demand. This finding extends earlier observations in locusts and cockroaches reporting co-activation of antagonistic muscles at the ThC and FTi joints in the early stance phase of level walking (Duch and Pflüger, 1995; Krauthamer and Fournier, 1978; Larsen et al., 1995). Moreover, it is consistent with the finding that antagonistic muscles at these joints show no co-activation in tethered animals walking on a slippery surface (Rosenbaum et al., 2010) – a situation in which legs do not have to be stabilized against gravity-induced collapse.

Transformation of muscle activity into movement

How does leg muscle activity relate to leg kinematics and leg dynamics during walking? In walking cockroaches, there is a linear relationship between the firing frequency of slow motor neurons

innervating extensor muscles at the CTr and FTi joints and joint angular velocity (Watson and Ritzmann, 1997; Watson et al., 2002b). Our multiunit recordings of muscles at the ThC joint prevented us from analyzing the firing frequency of identified motor neurons. Only the largest amplitude (putative fast) protractor units were individually identifiable (Fig. 4A, truncated). During swing, when the leg was uncoupled from the ground, the recruitment of these units was related to higher joint angular velocities (Fig. 4F). However, during stance, when the leg was mechanically coupled to the ground, muscle activity at the ThC joint did not directly reflect joint kinematics. During stance, the magnitude of muscle activity did not reflect joint angular velocity, but the net joint torque (Figs 3C and 4C). This finding highlights that the transformation of muscle activity into movement depends on the mechanical demands placed on the leg joint, which are phase and context dependent during walking. The transformation can be highly non-linear (Sponberg et al., 2011) given the complex contraction properties of insect muscle (Hooper and Weaver, 2000), passive forces of muscles and skeletal structures (Ache and Matheson, 2013; Hooper et al., 2009; Zakotnik et al., 2006), and mechanical coupling with other leg segments (Zajac, 1993). In our experiments, for example, the torque at the ThC joint reversed in sign during downhill walking, but protractor and retractor activity did not completely reverse. Rather, protractor activity occurred in the first half of stance and the main retractor activity was delayed (Fig. 4).

Motor control of level and incline walking

We found that muscle activity at the ThC joint is reliably adjusted to meet different mechanical demands during walking. What could be the underlying control? Previous studies on insects suggest that descending inputs from the brain mediate distinct kinematic patterns for turning (Gruhn et al., 2016; Martin et al., 2015) and obstacle climbing (Schütz and Dürr, 2011; Watson et al., 2002a,b). In our experiments, stick insects used a similar kinematic pattern across walking conditions (Fig. 2). In addition, protractor and retractor activity were adjusted primarily during the first half of stance after touch-down of the leg (Fig. 4), and with the first step of the leg on the incline (Fig. 5). Together, these findings could indicate that stick insects did not use distinct, inclination-specific motor programs, but instead adjusted leg muscle activity on a step-by-step basis using afferent inputs from leg proprioceptors.

One possibility is that muscle activity was adjusted based on load feedback from leg campaniform sensilla (Burrows and Pflüger, 1988; Pearson, 1972; Zill et al., 2012). These mechanoreceptors are located close to the leg joints and detect load as strain in the cuticle (Pringle, 1938; Zill et al., 2004). Our torque calculations show that the mechanical loads acting at the ThC and FTi joints differed substantially across walking conditions, suggesting that inputs from campaniform sensilla on the trochanter (Hofmann and Bässler, 1982; Schmitz, 1993) and tibia (Zill et al., 2011) differed too. For example, the resisted retraction torques during level and uphill walking should initially excite campaniform sensilla on the anterior side of the trochanter, whereas the resisted protraction torques during downhill walking should initially excite campaniform sensilla on the posterior side (Schmitz, 1993). In part, the muscle activity patterns observed in the present study could be explained assuming that the anterior group provides positive feedback to the retractor (resulting in retractor activity during the stance phase of level and uphill walking), whereas the posterior group provides positive feedback to the protractor (resulting in protractor activity during the stance phase of downhill walking). Load feedback from both groups of campaniform sensilla is known to affect muscle

activity at the ThC joint (Akay et al., 2004, 2007; Schmitz, 1993). However, the involvement of these groups in positive feedback pathways, as is known for campaniform sensilla on the dorsal trochanter (Zill et al., 2012), remains to be determined. In addition, load feedback cannot directly account for altered recruitment of protractor units during swing (Fig. 4F). This is because campaniform sensilla are only excited during stance, when leg muscle contractions are resisted (Zill et al., 2012). Therefore, it seems unlikely that simple load reflexes are sufficient to account for the adaptive changes in muscle activity observed in the present study.

Another possibility is that muscle activity was adjusted based on leg proprioceptors signaling leg position and movement. The finding that kinematics changed comparatively little across walking conditions might suggest that kinematic parameters are controlled. In a kinematic control scheme, muscle activity could depend on the mismatch between the actual and a desired, referent kinematic pattern. Any mismatch due to altered mechanical conditions could be determined based on signals from leg proprioceptors. For example, hair plates at proximal leg joints monitor the movement ranges of insect legs (Cruse et al., 1984; Markl, 1962; Schmitz, 1986; Wendler, 1964; Wong and Pearson, 1976), and chordotonal organs monitor the current position and movement of individual leg segments (Burns, 1974; Field and Matheson, 1998; Hofmann et al., 1985; Mamiya et al., 2018; Zill, 1985). Signals from these proprioceptors are critical for the spatial coordination of the leg (Bässler, 1977; Couzin-Fuchs et al., 2015; Mendes et al., 2013; Theunissen et al., 2014). The few changes in kinematics observed in the present study, such as the magnitude of the extension angle (Fig. 2H), do not contradict the idea of a kinematic control scheme. They could reflect that local control of joint angles does not always succeed completely, for example because of mechanical coupling with other legs. They could also indicate that a higher-level kinematic parameter is controlled. This conclusion is supported by previous studies showing that walking stick insects control walking speed (Cruse, 1985) and compensate for perturbations of body height and body tilt (Cruse, 1976a; Cruse et al., 1993; Diederich et al., 2002). Adjustments in muscle activity in response to altered mechanical demands might thus rely not only on local proprioceptive signals but also on proprioceptive signals from other legs (Ayali et al., 2015; Borgmann and Büschges, 2015). The transition from level to incline walking is an interesting scenario in this context. In the future, it might permit studying whether changes in muscle activity in one leg (hindleg) occur in response to changes in mechanical demands on another leg (front or middle leg).

In summary, we suggest that stick insects do not use distinct, inclination-specific motor programs during walking, but instead adjust leg muscle activity on a step-by-step basis so as to minimize changes in kinematics under different mechanical demands. Future work extending our measurements to other muscles, legs and more extreme inclinations will help to further probe this idea. For example, based on our torque calculations, we expect antagonistic muscle activity at the FTi joint to be adjusted similarly to that at the ThC joint. In addition, the reliable, characteristic changes in muscle activity described here might be suitable to evaluate the effects of sensory manipulations and determine which leg proprioceptors provide the critical sensory information for control.

Acknowledgements

We thank Yannick Günzel for help with data collection, Alessandro Moscatelli for advice on linear mixed models, Brigitta Otte-Eusterglering for maintaining our stick insect colony, and two anonymous reviewers for valuable comments.

Competing interests

The authors declare no competing or financial interests.

Author contributions

Conceptualization: C.J.D., J.S.; Methodology: C.J.D., V.D., J.S.; Formal analysis: C.J.D.; Investigation: C.J.D.; Resources: V.D., J.S.; Writing - original draft: C.J.D.; Writing - review & editing: C.J.D., V.D., J.S.; Visualization: C.J.D.; Supervision: V.D., J.S.; Funding acquisition: V.D., J.S.

Funding

This research was supported by the Cluster of Excellence Cognitive Interaction Technology 'CITEC' (EXC 277) at Bielefeld University, which is funded by the Deutsche Forschungsgemeinschaft (DFG).

Supplementary information

Supplementary information available online at <http://jeb.biologists.org/lookup/doi/10.1242/jeb.188748.supplemental>

References

- Ache, J. M. and Matheson, T. (2013). Passive joint forces are tuned to limb use in insects and drive movements without motor activity. *Curr. Biol.* **23**, 1418-1426.
- Akay, T., Haehn, S., Schmitz, J. and Büschges, A. (2004). Signals from load sensors underlie interjoint coordination during stepping movements of the stick insect leg. *J. Neurophysiol.* **92**, 42-51.
- Akay, T., Ludwar, B. C., Göritz, M. L., Schmitz, J. and Büschges, A. (2007). Segment specificity of load signal processing depends on walking direction in the stick insect leg muscle control system. *J. Neurosci.* **27**, 3285-3294.
- Altman, D. G. and Bland, J. M. (2011). How to obtain the *P* value from a confidence interval. *BMJ* **343**, d2304.
- Ayali, A., Couzin-Fuchs, E., David, I., Gal, O., Holmes, P. and Knebel, D. (2015). Sensory feedback in cockroach locomotion: current knowledge and open questions. *J. Comp. Physiol. A* **201**, 841-850.
- Bässler, U. (1977). Sensory control of leg movement in the stick insect *Carausius morosus*. *Biol. Cybern.* **25**, 61-72.
- Bässler, U. (1983). *Neural Basis of Elementary Behavior in Stick Insects*. Berlin: Springer.
- Bates, D., Mächler, M., Bolker, B. and Walker, S. (2015). Fitting linear mixed-effects models using lme4. *J. Stat. Softw.* **67**, 1-48.
- Bidaye, S. S., Bockemühl, T. and Büschges, A. (2018). Six-legged walking in insects: how CPGs, peripheral feedback, and descending signals generate coordinated and adaptive motor rhythms. *J. Neurophysiol.* **119**, 459-475.
- Borgmann, A. and Büschges, A. (2015). Insect motor control: methodological advances, descending control and inter-leg coordination on the move. *Curr. Opin. Neurobiol.* **33**, 8-15.
- Botev, Z. I., Grotowski, J. F. and Kroese, D. P. (2010). Kernel density estimation via diffusion. *Ann. Stat.* **38**, 2916-2957.
- Burns, M. D. (1974). Structure and physiology of the locust femoral chordotonal organ. *J. Insect Physiol.* **20**, 1319-1339.
- Burrows, M. and Pflüger, H. J. (1988). Positive feedback loops from proprioceptors involved in leg movements of the locust. *J. Comp. Physiol. A* **163**, 425-440.
- Büschges, A. and Gruhn, M. (2007). Mechanosensory feedback in walking: from joint control to locomotor patterns. *Adv. In Insect Phys.* **34**, 193-230.
- Carlson-Kuhta, P., Trank, T. V. and Smith, J. L. (1998). Forms of forward quadrupedal locomotion. II. A comparison of posture, hindlimb kinematics, and motor patterns for upslope and level walking. *J. Neurophysiol.* **79**, 1687-1701.
- Couzin-Fuchs, E., Gal, O., Holmes, P. and Ayali, A. (2015). Differential control of temporal and spatial aspects of cockroach leg coordination. *J. Insect Physiol.* **79**, 96-104.
- Cruse, H. (1976a). The control of body position in the stick insect (*Carausius morosus*), when walking over uneven surfaces. *Biol. Cybern.* **24**, 25-33.
- Cruse, H. (1976b). The function of the legs in the free walking stick insect, *Carausius morosus*. *J. Comp. Physiol. A* **112**, 235-262.
- Cruse, H. (1979). The control of the anterior extreme position of the hindleg of a walking insect, *Carausius morosus*. *Physiol. Entomol.* **4**, 121-124.
- Cruse, H. (1985). Which parameters control the leg movement of a walking insect? I. Velocity control during the stance phase. *J. Exp. Biol.* **116**, 343-355.
- Cruse, H., Dean, J. and Suilmann, M. (1984). The contributions of diverse sense organs to the control of leg movement by a walking insect. *J. Comp. Physiol. A* **154**, 695-705.
- Cruse, H., Schmitz, J., Braun, U. and Schweins, A. (1993). Control of body height in a stick insect walking on a treadmill. *J. Exp. Biol.* **181**, 141-155.
- Dallmann, C. J., Dürr, V. and Schmitz, J. (2016). Joint torques in a freely walking insect reveal distinct functions of leg joints in propulsion and posture control. *Proc. R. Soc. B Biol. Sci.* **283**, 20151708.
- Dallmann, C. J., Hoinville, T., Dürr, V. and Schmitz, J. (2017). A load-based mechanism for inter-leg coordination in insects. *Proc. R. Soc. B Biol. Sci.* **284**, 20171755.

- Dean, J. and Wendler, G. (1983). Stick insect locomotion on a walking wheel: interleg coordination of leg position. *J. Exp. Biol.* **103**, 75-94.
- Diederich, B., Schumm, M. and Cruse, H. (2002). Stick insects walking along inclined surfaces. *Integr. Comp. Biol.* **42**, 165-173.
- Donelan, J. M., McVea, D. A. and Pearson, K. G. (2009). Force regulation of ankle extensor muscle activity in freely walking cats. *J. Neurophysiol.* **101**, 360-371.
- Duch, C. and Pflüger, H. J. (1995). Motor patterns for horizontal and upside down walking and vertical climbing in the locust. *J. Exp. Biol.* **198**, 1963-1976.
- Dürr, V., Theunissen, L. M., Dallmann, C. J., Hoinville, T. and Schmitz, J. (2018). Motor flexibility in insects: adaptive coordination of limbs in locomotion and near-range exploration. *Behav. Ecol. Sociobiol.* **72**, 15.
- Field, L. H. and Matheson, T. (1998). Chordotonal organs of insects. *Adv. In Insect Phys.* **27**, 1-228.
- Goldammer, J., Büschges, A. and Schmidt, J. (2012). Motoneurons, DUM cells, and sensory neurons in an insect thoracic ganglion: a tracing study in the stick insect *Carausius morosus*. *J. Comp. Neurol.* **520**, 230-257.
- Goldman, D. I., Chen, T. S., Dudek, D. M. and Full, R. J. (2006). Dynamics of rapid vertical climbing in cockroaches reveals a template. *J. Exp. Biol.* **209**, 2990-3000.
- Gottschall, J. S. and Nichols, T. R. (2011). Neuromuscular strategies for the transitions between level and hill surfaces during walking. *Philos. Trans. R. Soc. B* **366**, 1565-1579.
- Graham, D. (1985). Pattern and control of walking in insects. *Adv. In Insect Phys.* **18**, 32-140.
- Gregor, R. J., Smith, D. W. and Prilutsky, B. I. (2006). Mechanics of slope walking in the cat: quantification of muscle load, length change, and ankle extensor EMG patterns. *J. Neurophysiol.* **95**, 1397-1409.
- Gruhn, M., Rosenbaum, P., Bockemühl, T. and Büschges, A. (2016). Body side-specific control of motor activity during turning in a walking animal. *eLife* **5**, e13799.
- Guschlbauer, C., Scharstein, H. and Büschges, A. (2007). The extensor tibiae muscle of the stick insect: biomechanical properties of an insect walking leg muscle. *J. Exp. Biol.* **210**, 1092-1108.
- Hofmann, T. and Bässler, U. (1982). Anatomy and physiology of trochanteral campaniform sensilla in the stick insect, *Cuniculina impigra*. *Physiol. Entomol.* **7**, 413-426.
- Hofmann, T., Koch, U. T. and Bässler, U. (1985). Physiology of the femoral chordotonal organ in the stick insect, *Cuniculina impigra*. *J. Exp. Biol.* **114**, 207-223.
- Hooper, S. L. and Büschges, A. (2017). *Neurobiology of Motor Control: Fundamental Concepts and New Directions*. Wiley.
- Hooper, S. L. and Weaver, A. L. (2000). Motor neuron activity is often insufficient to predict motor response. *Curr. Opin. Neurobiol.* **10**, 676-682.
- Hooper, S. L., Guschlbauer, C., von Uckermann, G. and Büschges, A. (2007). Slow temporal filtering may largely explain the transformation of stick insect (*Carausius morosus*) extensor motor neuron activity into muscle movement. *J. Neurophysiol.* **98**, 1718-1732.
- Hooper, S. L., Guschlbauer, C., Blümel, M., Rosenbaum, P., Gruhn, M., Akay, T. and Büschges, A. (2009). Neural control of unloaded leg posture and of leg swing in stick insect, cockroach, and mouse differs from that in larger animals. *J. Neurosci.* **29**, 4109-4119.
- Janshen, L., Santuz, A., Ekizos, A. and Arampatzis, A. (2017). Modular control during incline and level walking in humans. *J. Exp. Biol.* **220**, 807-813.
- Krauthamer, V. and Fournier, C. R. (1978). Locomotor activity in the extensor and flexor tibiae of the cockroach, *Periplaneta americana*. *J. Insect Physiol.* **24**, 813-819.
- Larsen, G. S., Frazier, S. F., Fish, S. E. and Zill, S. N. (1995). Effects of load inversion in cockroach walking. *J. Comp. Physiol. A* **176**, 229-238.
- Lay, A. N., Hass, C. J. and Gregor, R. J. (2006). The effects of sloped surfaces on locomotion: a kinematic and kinetic analysis. *J. Biomech.* **39**, 1621-1628.
- Lay, A. N., Hass, C. J., Nichols, R. T. and Gregor, R. J. (2007). The effects of sloped surfaces on locomotion: an electromyographic analysis. *J. Biomech.* **40**, 1276-1285.
- Leroux, A., Fung, J. and Barbeau, H. (2002). Postural adaptation to walking on inclined surfaces: I. Normal strategies. *Gait Posture* **15**, 64-74.
- Mamiya, A., Gurung, P. and Tuhill, J. C. (2018). Neural coding of leg proprioception in *Drosophila*. *Neuron* **100**, 636-650.e6.
- Markl, H. (1962). Borstenfelder an den Gelenken als Schweresinnesorgane bei Ameisen und anderen Hymenopteren. *Z. Vgl. Physiol.* **45**, 475-569.
- Martin, J. P., Guo, P., Mu, L., Harley, C. M. and Ritzmann, R. E. (2015). Central-complex control of movement in the freely walking cockroach. *Curr. Biol.* **25**, 2795-2803.
- Mendes, C. S., Bartos, I., Akay, T., Márka, S. and Mann, R. S. (2013). Quantification of gait parameters in freely walking wild type and sensory deprived *Drosophila melanogaster*. *eLife* **2**, e00231.
- Mendes, C. S., Rajendren, S. V., Bartos, I., Márka, S. and Mann, R. S. (2014). Kinematic responses to changes in walking orientation and gravitational load in *Drosophila melanogaster*. *PLoS ONE* **9**, e109204.
- Orlovsky, G. N., Deliagina, T. G. and Grillner, S. (1999). *Neuronal Control of Locomotion: From Mollusc to Man*. Oxford, UK: Oxford University Press.
- Pearson, K. G. (1972). Central programming and reflex control of walking in the cockroach. *J. Exp. Biol.* **56**, 173-193.
- Pearson, K. G. (1995). Proprioceptive regulation of locomotion. *Curr. Opin. Neurobiol.* **5**, 786-791.
- Pringle, J. W. S. (1938). Proprioception in insects. II. The action of the campaniform sensilla on the legs. *J. Exp. Biol.* **15**, 114-131.
- Prochazka, A. (1996). Proprioceptive feedback and movement regulation. In *Handbook of Physiology, Exercise: Regulation and Integration of Multiple Systems* (ed. L. B. Rowell and J. T. Shepherd), pp. 89-127. American Physiological Society.
- Rosenbaum, P., Wosnitzer, A., Büschges, A. and Gruhn, M. (2010). Activity patterns and timing of muscle activity in the forward walking and backward walking stick insect *Carausius morosus*. *J. Neurophysiol.* **104**, 1681-1695.
- Schmitz, J. (1986). Properties of the feedback system controlling the coxa-trochanter joint in the stick insect *Carausius morosus*. *Biol. Cybern.* **55**, 35-42.
- Schmitz, J. (1993). Load-compensating reactions in the proximal leg joints of stick insects during standing and walking. *J. Exp. Biol.* **33**, 15-33.
- Schütz, C. and Dürr, V. (2011). Active tactile exploration for adaptive locomotion in the stick insect. *Philos. Trans. R. Soc. B* **366**, 2996-3005.
- Seidl, T. and Wehner, R. (2008). Walking on inclines: how do desert ants monitor slope and step length. *Front. Zool.* **5**, 8.
- Smith, J. L., Carlson-Kuhta, P. and Trank, T. V. (1998). Forms of forward quadrupedal locomotion. III. A comparison of posture, hindlimb kinematics, and motor patterns for downslope and level walking. *J. Neurophysiol.* **79**, 1702-1716.
- Spirito, C. P. and Mushrush, D. L. (1979). Interlimb coordination during slow walking in the cockroach. I. Effects of substrate alterations. *J. Exp. Biol.* **79**, 233-243.
- Sponberg, S., Spence, A. J., Mullens, C. H. and Full, R. J. (2011). A single muscle's multifunctional control potential of body dynamics for postural control and running. *Philos. Trans. R. Soc. B* **366**, 1592-1605.
- Szczecinski, N. S., Bockemühl, T., Chockley, A. S. and Büschges, A. (2018). Static stability predicts the continuum of interleg coordination patterns in *Drosophila*. *J. Exp. Biol.* **221**, jeb189142.
- Theunissen, L. M. and Dürr, V. (2013). Insects use two distinct classes of steps during unrestrained locomotion. *PLoS ONE* **8**, e85321.
- Theunissen, L. M., Vikram, S. and Dürr, V. (2014). Spatial co-ordination of foot contacts in unrestrained climbing insects. *J. Exp. Biol.* **217**, 3242-3253.
- Tuhill, J. C. and Wilson, R. I. (2016). Mechanosensation and adaptive motor control in insects. *Curr. Biol.* **27**, R1022-R1038.
- Wahl, V., Pfeffer, S. E. and Wittlinger, M. (2015). Walking and running in the desert ant *Cataglyphis fortis*. *J. Comp. Physiol. A* **201**, 645-656.
- Watson, J. T. and Ritzmann, R. E. (1997). Leg kinematics and muscle activity during treadmill running in the cockroach, *Blaberus discoidalis*: I. Slow running. *J. Comp. Physiol. A* **182**, 11-22.
- Watson, J. T., Ritzmann, R. E., Zill, S. N. and Pollack, A. J. (2002a). Control of climbing behavior in the cockroach, *Blaberus discoidalis*. I. Kinematics. *J. Comp. Physiol. A* **188**, 39-53.
- Watson, J. T., Ritzmann, R. E. and Pollack, A. J. (2002b). Control of climbing behavior in the cockroach, *Blaberus discoidalis*. II. Motor activities associated with joint movement. *J. Comp. Physiol. A* **188**, 55-69.
- Weihmann, T. and Blickhan, R. (2009). Comparing inclined locomotion in a ground-living and a climbing ant species: sagittal plane kinematics. *J. Comp. Physiol. A* **195**, 1011-1020.
- Wendler, G. (1964). Laufen und Stehen der Stabheuschrecke *Carausius morosus*: Sinnesborstenfelder in den Beimgelenken als Glieder von Regelkreisen. *Z. Vgl. Physiol.* **48**, 198-250.
- Wöhrl, T., Reinhardt, L. and Blickhan, R. (2017). Propulsion in hexapod locomotion: how do desert ants traverse slopes? *J. Exp. Biol.* **220**, 1618-1625.
- Wong, R. K. and Pearson, K. G. (1976). Properties of the trochanteral hair plate and its function in the control of walking in the cockroach. *J. Exp. Biol.* **64**, 233-249.
- Zajac, F. E. (1993). Muscle coordination of movement: a perspective. *J. Biomech.* **26**, 109-124.
- Zakotnik, J., Matheson, T. and Dürr, V. (2006). Co-contraction and passive forces facilitate load compensation of aimed limb movements. *J. Neurosci.* **26**, 4995-5007.
- Zill, S. N. (1985). Plasticity and proprioception in insects. I. Responses and cellular properties of individual receptors of the locust metathoracic femoral chordotonal organ. *J. Exp. Biol.* **116**, 435-461.
- Zill, S. N., Schmitz, J. and Büschges, A. (2004). Load sensing and control of posture and locomotion. *Arthropod Struct. Dev.* **33**, 273-286.
- Zill, S. N., Büschges, A. and Schmitz, J. (2011). Encoding of force increases and decreases by tibial campaniform sensilla in the stick insect, *Carausius morosus*. *J. Comp. Physiol. A* **197**, 851-867.
- Zill, S. N., Schmitz, J., Chaudhry, S. and Büschges, A. (2012). Force encoding in stick insect legs delineates a reference frame for motor control. *J. Neurophysiol.* **108**, 1453-1472.

Table S1. Kinematic parameters for level walking with and without the EMG backpack

Kinematic parameter	control	EMG backpack
Pro. swing (deg)	-33.0±4.9	-38.6±2.8 [-12]
Pro. stance (deg)	-42.8±6.1	-42.9±3.8 [<1]
Sup. swing (deg)	1.8±5.3	-0.2±5.1 [-8]
Sup. stance (deg)	-0.3±5.2	-0.1±4.6 [1]
Lev. swing (deg)	31.8±7.1	30.9±6.5 [-3]
Lev. stance (deg)	27.1±2.8	23.6±3.7 [-11]
Ext. swing (deg)	110.5±4.0	110.2±5.5 [<1]
Ext. stance (deg)	88.2±4.7	86.8±3.5 [-2]

Values are means±s.d. of animal means (control, 5 animals, 10 steps per animal; EMG backpack, same animals, 18-33 steps per animal). Values in brackets indicate differences from level walking as a percentage of the range of the parameter (peak-to-peak amplitude of the parameter's mean time course) during the step cycle of control steps. Angles are net values averaged over each phase of the step cycle. Pro., protraction angle; Sup., supination angle; Lev., levation angle; Ext., extension angle. See Fig. 1B for angle conventions.

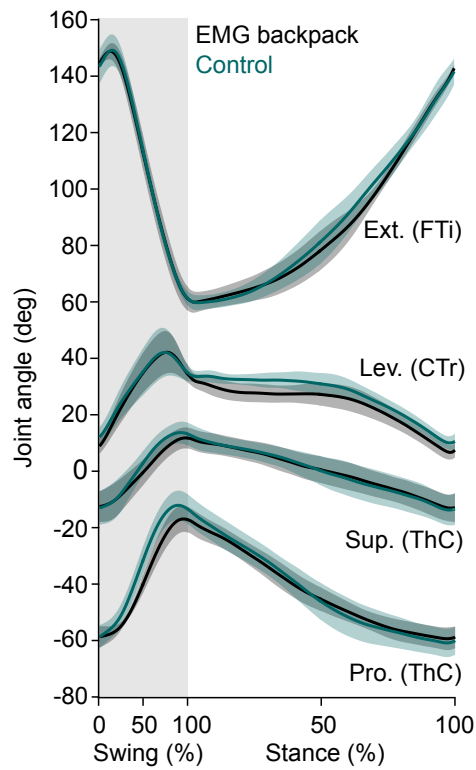


Fig. S1. Effects of the EMG backpack on hind leg kinematics. Joint angles of the hind leg during level walking normalized to swing and stance duration. Lines and error bands show means and 95% confidence intervals of animal means. Black lines show data with EMG backpack attached and electrodes implanted (5 animals, 18-33 steps per animal; same as black lines in Fig. 2H). Green lines show control data recorded from the same animals prior to backpack attachment and electrode implantation (5 animals, 10 steps per animal).